Bull. Mater. Sci., Vol. 33, No. 2, April 2010, pp. 89–95. © Indian Academy of Sciences.

Rapid growth of nanotubes and nanorods of würtzite ZnO through microwave-irradiation of a metalorganic complex of zinc and a surfactant in solution

SANJAYA BRAHMA[1], KALYA JAGANNATHA RAO* and SRINIVASARAO SHIVASHANKAR[1,2]

Solid State and Structural Chemistry Unit, [1]Materials Research Centre, [2]Centre for Excellence in Nanoelectronics, Indian Institute of Science, Bangalore 560 012, India

MS received 9 February 2010

Abstract. Large quantities of single-crystalline ZnO nanorods and nanotubes have been prepared by the microwave irradiation of a metalorganic complex of zinc, in the presence of a surfactant. The method is simple, fast, and inexpensive (as it uses a domestic microwave oven), and yields pure nanostructures of the hexagonal würtzite phase of ZnO in min, and requires no conventional templating. The ZnO nanotubes formed have a hollow core with inner diameter varying from 140–160 nm and a wall of thickness, 40–50 nm. The length of nanorods and nanotubes varies in the narrow range of 500–600 nm. These nanostructures have been characterized by X-ray diffraction (XRD), scanning electron microscopy (SEM), transmission electron microscopy (TEM), and selected area electron diffraction (SAED). The ZnO nanorods and nanotubes are found by SAED to be single-crystalline. The growth process of ZnO nanorods and nanotubes has been investigated by varying the surfactant concentration and microwave irradiation time. Based on the various results obtained, a tentative and plausible mechanism for the formation of ZnO nanostructures is proposed.

Keywords. Nanostructures; crystal growth; electron microscopy.

1. Introduction

Control of the shape and orientation of nano crystallites of oxides, with various morphologies such as wires, rods, belts, and tubes, has attracted much attention in the literature. This is because it is important to understand the effects of morphology, dimensionality, and size on their physical and chemical properties, particularly in view of their application in optoelectronic devices. Specificity of semiconductor nanostructures are of great interest for future electronic and photonic devices (Arakawa and Sakaki 1970; Weisbuch *et al* 2000; Bukowski and Simmons 2002). Zinc oxide (ZnO), is an oxide semiconductor with wide direct band gap (3·37 eV) and large exciton binding energy (60 meV), and is an excellent candidate material for studies in modern nanoelectronics and photonics. ZnO nanostructures possess excellent potential for applications in short-wavelength light-emitting devices (Huang *et al* 2001), field-emission devices (Lee *et al* 2002), solar cells (Keis *et al* 2002), and sensors (Hu *et al* 2003). Various ZnO nanostructures have been realized, such as nanodots (Kim *et al* 2002), nanowires, nanorods, nanoribbons (Pan *et al* 2001; Wu and Liu 2002; Lee *et al* 2004; Zou *et al* 2006; Jung *et al* 2007), nanobridges and nanonails, nanowalls (Lao *et al* 2003; Ng *et al* 2003), and nanotubes (Xing *et al* 2003; Zhang *et al* 2004; Jian *et al* 2005; Wu *et al* 2006; Zhou *et al* 2006). Several methods for obtaining ZnO nanostructures have been developed, such as thermal evaporation (Huang *et al* 2001; Lee *et al* 2002, 2004; Lao *et al* 2003; Ng *et al* 2003; Xing *et al* 2003), metalorganic chemical vapour deposition (MOCVD) (Kim *et al* 2002; Wu and Liu 2002; Zhang *et al* 2004), sonochemical synthesis (Jung *et al* 2007), plasma-assisted molecular beam epitaxy (Jian *et al* 2005), solution-phase approach (Wu *et al* 2006) and microwave heating (Zhou *et al* 2006). All these methods employ either a vapour–liquid–solid (VLS) process or vapour–solid (VS) process to grow the nanostructures, and require long periods of processing. Therefore, we consider that it is worthwhile to develop methods of preparing nanomaterials and nanostructures, which work at low temperatures, are fast, and cost-effective. We have investigated the potential of using microwave-assisted chemical reactions to obtain nanostructures of oxides, and report here on the synthesis of ZnO nanorods and nanotubes from a metalorganic complex of zinc, by irradiating it with microwaves. The effect of the variation of parameters, such as irradiation period and surfactant concentration, on the formation of nanostructures of ZnO has

*Author for correspondence (kjrao@sscu.iisc.ernet.in)

also been investigated. Apart from the simplicity of the equipment it calls for and its speed, the method described below has the advantage of yielding single-crystalline, well-faceted, hexagonal nanorods and nanotubes of ZnO without the need for any template. All the nanorods and nanotubes obtained in this process are hexagonal, bearing the same crystallographic orientation. After the present work was completed, we have learned of the work of Kong *et al* (2007) wherein ZnO nanotubes have been synthesized in a microwave-assisted method, without using templates. However, the process requires as much as 40 min, and the yield of the process is not reported. More recently, Bilecka *et al* (2008) reported the rapid synthesis of nanocrystals of oxides such as ZnO, but not of their nanotubes or nanorods.

2. Experimental

The synthesis of ZnO nanostructures involves the β-diketonate complex of zinc, viz. Zn(II) acetylacetonate ($C_{10}H_{14}O_4Zn$), often denoted by Zn(*acac*)$_2$, a crystalline solid at room temperature. The schematic molecular structure of Zn(*acac*)$_2$ is given in figure 1, showing the direct Zn–O bonds present in the complex, making it a suitable precursor for the synthesis of ZnO. In the present procedure, one gram of high-purity Zn(II) acetylacetonate is taken in a round-bottomed flask and dissolved in 40 ml of ethanol (99·9%, HPLC grade), and stirred for 15 min. A solution of the surfactant polyvinyl pyrrolidone (PVP, mol.wt. 360,000) in double-distilled water is prepared (0·3 g PVP in 40 ml water) and added to the solution containing Zn(*acac*)$_2$, followed by 15 min of stirring. (The surfactant was added to prevent agglomeration of particles that result from microwave irradiation.) The solution so obtained in the round-bottomed flask was placed in a domestic-type microwave oven (2·45 GHz, power variable from 160–800 W). Both the composition of the solutions prepared and the parameters of the microwave irradiation were varied. The conditions employed to prepare samples discussed below are listed in table 1. It may be noted that the microwave oven was modified to accommodate a water-cooled condenser (reflux system). The modification was such that the condenser was projected on the top of the microwave oven.

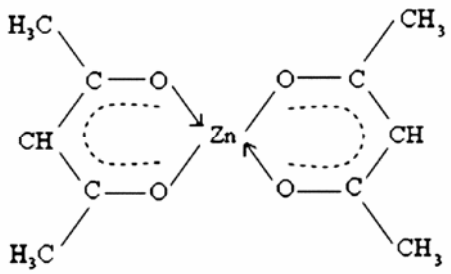

Figure 1. The schematic molecular structure of Zn(*acac*)$_2$.

Microwave irradiation of the solution was found to result in a cloudy and white colloidal suspension. Centrifugation of this suspension, followed by washing with acetone and distilled water, yielded a fine white powder. The powder was heated for a few minutes in air at 400°C in order to remove the surfactant.

All the samples were characterized by powder XRD (Philips diffractometer, Model 3710 MPD Cu-K_α radiation). XRD patterns were recorded from 20° to 80° (2θ) with a scanning step of one degree per minute. The size distribution and morphology of the particles in the samples were analyzed by field emission scanning electron microscopy (FE-SEM SIRION XL-40) and transmission electron microscopy (TEM-TECNAI F-30). Selected area electron diffraction (SAED) was carried out in the TEM to analyse the structure of individual fine particles in the samples. Elemental analysis was carried out by an energy-dispersive X-ray analyser attached to SEM and TEM.

3. Results and discussion

It is found that microwave irradiation for less than ~25 s produces incompletely reacted amorphous material. The powder XRD pattern of a sample resulting from 30 s of irradiation (800 W) is shown in figure 2a, which clearly indicates that the sample is well crystallized. All the diffraction peaks could be indexed to ZnO of the hexagonal würtzite structure (JCPDS File No – 05-0664). The XRD data yielded lattice constants of a = 3·248 Å and c = 5·203 Å (JCPDS File No – 05-0664). The absence of any other diffraction peaks confirms that the reaction was complete and the product, hexagonal ZnO, was phase pure. The nanoparticles were spherical in shape and their sizes exhibited a fairly narrow distribution centred at ~40 nm, as revealed in the SEM micrograph (figure 2b).

As the duration of irradiation (at 800 W) was increased, the morphology of the ZnO crystallites changed markedly, with characteristic hexagonal shapes appearing after about 1 min (figure 3a), longer durations resulted in the formation of distinct hexagonal rods and hollow tubes, with rods outnumbering tubes (figure 3b). Microwave irradiation for 5 min (at 800 W) resulted in a harvest of well-faceted, hexagonal rods and tubes of ZnO (figure 3c). The observed rod diameters varied between 80 and 100 nm, with lengths up to 500–600 nm. The wall thickness of the hollow ZnO structures was about 40 nm, with their inner diameter in the range of 140–160 nm. These structures have, therefore, been designated by us as nanorods and nanotubes of ZnO. It can clearly be seen in figures 3b and 3c that the nanostructures display uniform diameters along the normal to the hexagon. The distinctive feature of the tubes is that they possess smooth faces and regular hexagonal cross sections, although no

Table 1a. Experimental conditions used for the preparation of ZnO nanostructures: Variation of PVP concentration, keeping other parameters fixed.

Microwave power	Microwave irradiation time	PVP conc. in ethanol (g/40 ml)	Nanostructures obtained
800 W	5 min	0·1	Some irregularly shaped nanoparticles
		0·3	Nanorods and nanotubes
		0·5	Nanorods and nanotubes
		1	Nanorods and nanotubes

Table 1b. Experimental conditions used for the preparation of ZnO nanostructures. Variation of microwave irradiation time, keeping other parameters fixed.

Microwave power	Microwave irradiation time	PVP conc. in ethanol (g/40 ml)	Nanostructures obtained
800 W	1 min	0·3	Nanorods and nanotubes
	2 min		Nanorods and nanotubes
	5 min		Nanorods and nanotubes

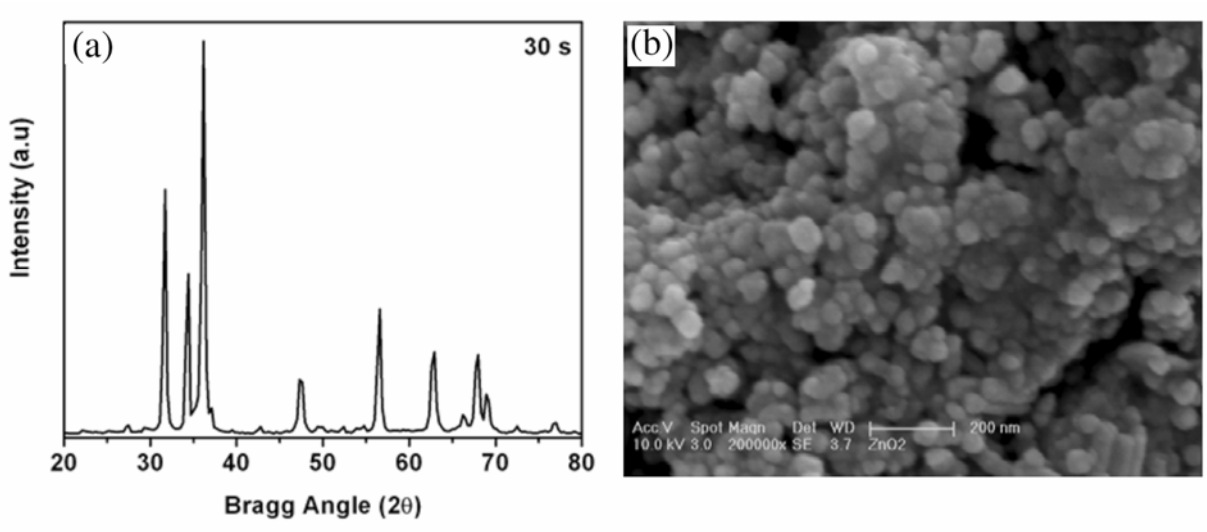

Figure 2. (**a**) X-ray diffraction pattern (XRD) of ZnO nanoparticles prepared after 30 s of microwave irradiation and (**b**) scanning electron micrograph (SEM) of ZnO nanoparticles.

conventional template has been used in their liquid phase preparation. The XRD pattern of the '5 min sample' is given in figure 3d, showing sharp reflections, consistent with the SEM data.

The morphology and crystallinity of individual nanostructures—both nanorods and nanotubes—were investigated further using TEM. The selected area electron diffraction (SAED) pattern of a single nanorod of ZnO is shown in figure 4a. Bright diffraction spots corresponding to all the crystal planes of the würtzite structure, are clearly visible. The nanorods are therefore single crystals of high quality. The spot pattern has been indexed and the zone axis determined as shown. A close examination of the diffraction pattern reveals that the as-prepared ZnO nanorods are covered by $\pm\{10\bar{1}l\}$ facets i.e. the 'side surfaces' of the rods are formed by the family of ZnO $(10\bar{1}0)$ planes, and the zone axis corresponds to $[2\bar{1}\bar{1}0]$ (Edington 1976). The appearance of the diffraction spots such as $(0\ 0\ 0\ 2n+1)$ (n is an integer) is due to the double diffraction effect. For example, the (0001) diffraction spots [between (0002) and the central spot] are due to the double diffraction from $(10\bar{1}0)$ and $(10\bar{1}1)$ planes (Edington 1976). Thus the SAED pattern confirms that the preferred growth direction of as-prepared ZnO nanorods is (0001). The SAED pattern of a single nanotube is shown in figure 4b, confirming that the nanotubes are also single crystals of würtzite, with the [0001] orientation. In the SAED pattern, it is noticed that each spot is associated with an additional spot, which is attributable to the shape of the nanotube.

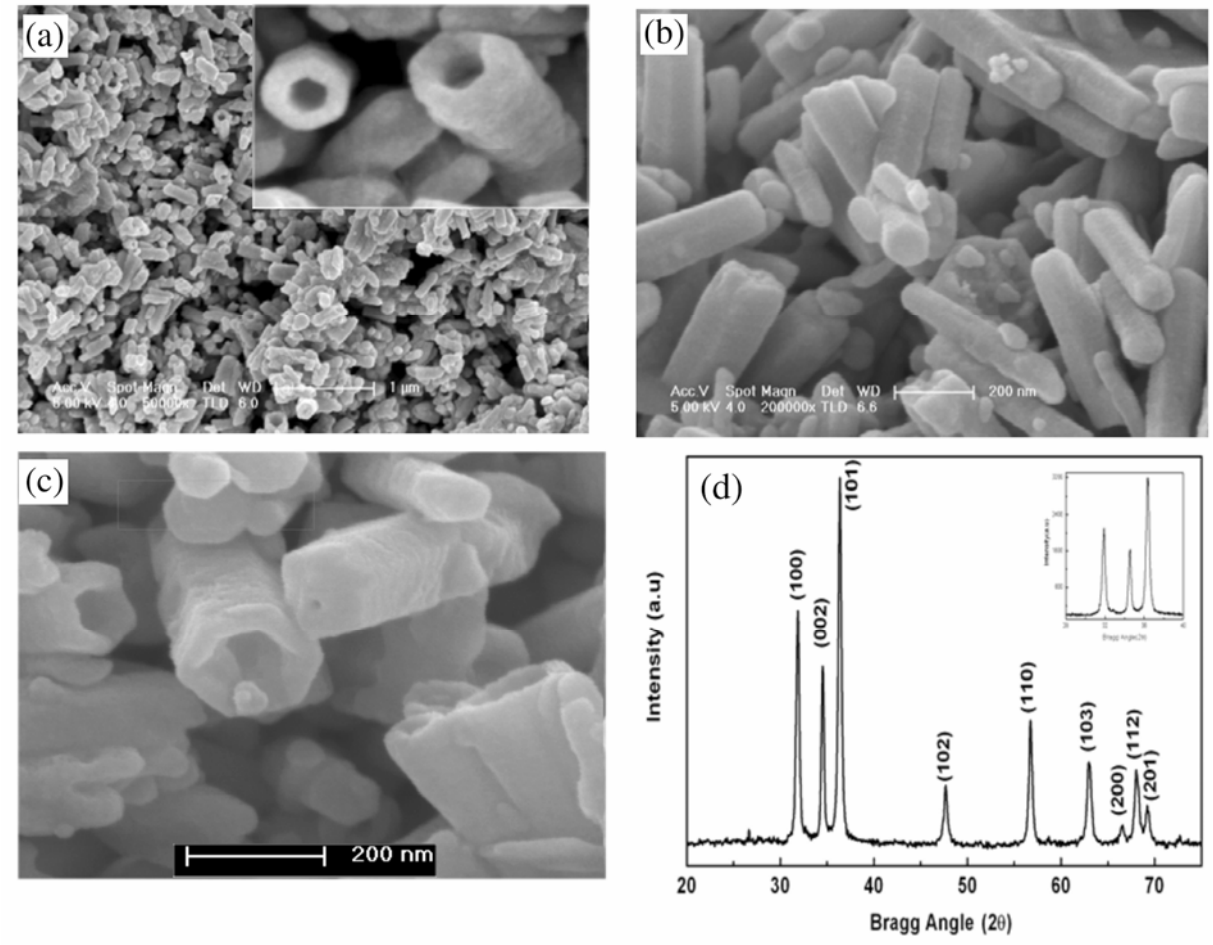

Figure 3. (**a**) SEM of ZnO nanorods and nanotubes prepared after 1 min of microwave irradiation (inset shows higher magnification), (**b**) SEM of ZnO nanorods, (**c**) SEM of ZnO nanotubes and (**d**) XRD pattern of ZnO nanorods and nanotubes obtained after 5 min of microwave irradiation.

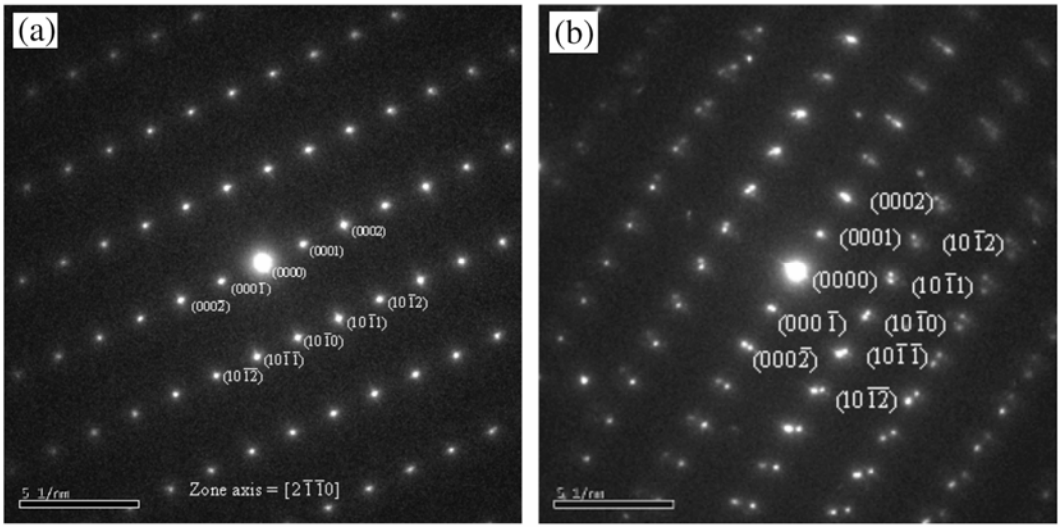

Figure 4. (**a**) Selected area electron diffraction pattern of a single nanorod and (**b**) selected area electron diffraction pattern of a single nanotube.

3.1 *Growth kinetics*

To investigate the formation and growth of the ZnO nanorods and nanotubes, a number of growth runs were conducted, by varying the PVP concentration and the duration of microwave irradiation. The experimental conditions are detailed in tables 1(a) and 1(b). The approach was first to optimize the PVP concentration, keeping microwave power and microwave irradiation time fixed, so that well-defined nanostructures were obtained. Experiments revealed that 0·4 wt% (0·3 g in the mixture of 40 ml of C_2H_5OH and 40 ml of water) is the minimum concentration of PVP to obtain nanorods and nanotubes. Similarly minimum irradiation time was found to be just 1 min for the formation of ZnO nanorods and nanotubes as already noted. It was observed that, higher concentration of PVP (>0·4%) and irradiation duration of more than 1 min did not affect the size and shape of the resulting nanostructures.

3.2 *A possible mechanism for formation of ZnO nanostructures*

We recall here a few important observations: (i) three different nanostructures are formed in the microwave irradiation process: nanoparticles which are spheroidal, nanorods, and nanotubes, (ii) nanoparticles are observed only when microwave irradiation is performed for <1 min, (iii) exposure to microwaves for 1 min or longer leads to the formation of only nanotubes and nanorods, (iv) statistically, we note that nanorods form in greater abundance than nanotubes, and this observation is independent of the time of exposure as long as it is more than 1 min, (v) even more significantly nanorods and nanotubes are essentially of the same length and (vi) the tubes have hexagonal cross-sections, and the rods are faceted. We propose the following tentative mechanism for the formation of the observed nanostructures, which is also consistent with the above observations.

The PVP solution in water, used in the synthesis, was prepared by a gentle procedure (no vigorous stirring). A large proportion of the linear PVP strands are thus prodded to organize themselves into PVP bundles. The strands in the bundle are held together by H_2O through hydrogen bonding to C=O on the pyrrolidone ring (figure 5a). Such extensive inter-strand hydrogen bonding is possible because of the free rotation of the pyrrolidone ring on the C–N bond. It is in effect a mild and localized gelation, which results in the formation of numerous PVP bundles suspended in water. When the ethanolic solution of Zn(*acac*)$_2$ is added to such a suspension of PVP bundles, we envisage the formation of at least three distinct structural entities in the solution: (i) the larger PVP bundles get completely covered by layers of Zn(*acac*)$_2$ molecules, (ii) smaller PVP bundles first get smeared with Zn(*acac*)$_2$ molecules and, subsequently, these bundles pull together in such a way as to form PVP tubes filled

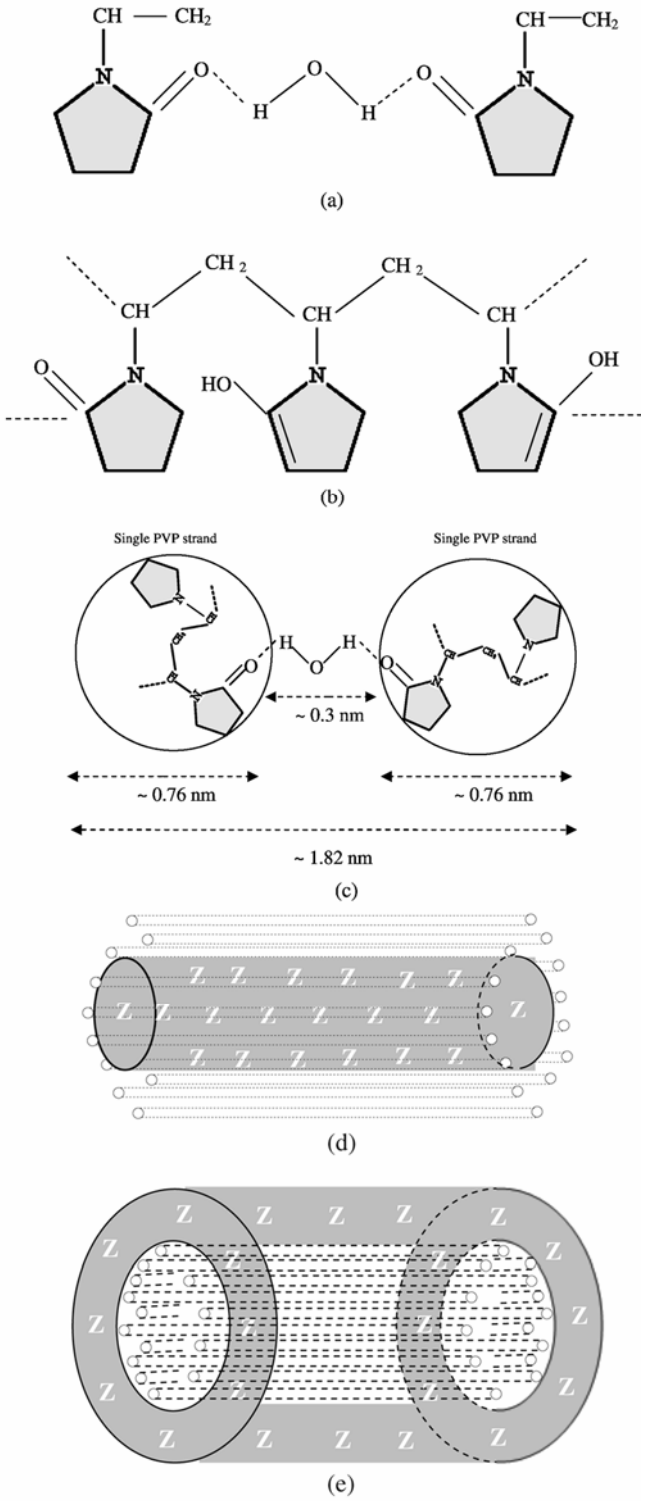

Figure 5. (**a**) Hydrogen bonding between PVP and water, (**b**) schematic structure of the PVP molecule, (**c**) two PVP strands connected by a H_2O molecule, (**d**) ZnO nanorod growth inside PVP tubes formed by PVP strands and (**e**) ZnO nanotube growth on PVP bundles formed by PVP strands.

with Zn(*acac*)$_2$ molecules and (iii) the unassociated free strands of PVP organize themselves into spheroidal droplets with encapsulated Zn(*acac*)$_2$ molecules.

Upon irradiation, microwaves are absorbed by both water and Zn(*acac*)$_2$. The response to irradiation of the three structural formations is considered to be as follows.

In the first case, where Zn(*acac*)$_2$ is present as a cylindrical sheath around the PVP bundle, Zn(*acac*)$_2$ decomposes to form zinc oxide. Water involved in hydrogen bonding in the PVP bundles is also activated. As the water molecules in the bundle escape, PVP strands get closer (shrinking of the bundle diameter). Upon further irradiation, PVP undergoes cross linking through condensation of the enolic forms of pyrrolidone rings (figure 5b). Cross-linking of the PVP strands and the shrinking of the bundles helps the cylindrical shell of ZnO to easily delink from the polymeric core. This results in the formation of ZnO tubes.

In the second case, the situation is somewhat inverted with respect to the first. Formation of ZnO takes place in the core (figure 5c). Since ZnO has a volume which is lower than that of Zn(*acac*)$_2$, the core shrinks. The bundles of cross-polymerized PVP (known as PVPP) also shrink but will result in reducing the thickness of the outer sheath. Therefore, the sheath and the inner rod like core get separated. This results in the formation of rods.

In the third situation of individual droplets, Zn(*acac*)$_2$ decomposes leading to ZnO particles which remain enclosed in cross-linked PVP shells (figure 5d).

In the above mechanism the lengths of the tubes and rods formed eventually are expected to be nearly equal to the lengths of PVP strands. To examine this aspect, we proceed as follows. The monomeric unit in PVP has the molecular weight of 111, and the PVP employed here as the surfactant has a molecular weight of 360,000. Therefore, there are ~3200 monomer units in each PVP strand, the monomeric units being connected in a zig-zag chain. Assuming the C–C–C angle in ---CH_2–CH–CH_2--- link to be tetrahedral the length of a PVP is easily seen to be ~500 nm. It is gratifying to note that the observed lengths of tubes and rods are very close and ~500 nm. Encouraged by this consistency, we have estimated the number of PVP strands likely to be present in the bundle. Allowing for a random distribution of the dihedral angles along the polymer axis, a PVP strand will have an effective diameter of 1·52 nm. It is the diameter of the cylindrical cross-section, when two such PVP 'cylinders' (figure 5c) are connected by a H_2O molecule forming two hydrogen bonds. The two 'cylinders' are now bound at a distance of 0·3 nm. Again since the H-bonding itself is in random directions, the randomly H-bonded units will all be located around the central cylinder. The 'super cylindrical' assembly possesses an effective diameter of 2·88 nm. Further, such 'supercylinders' are assumed to be organized into yet bigger cylindrical bundle with a near circular cross-section incorporating the H-bonding water molecules. The radius of such a bundle would be ~50 nm. In such a cylindrical bundle, there would be about 900 PVP strands. Such a bundle can give rise to nanotubes of ZnO, which has an inner diameter of about ~80–100 nm. The tubes are, however, hexagonal in cross-section which is likely to be a result of two factors operating in the system. Formation of ZnO takes place first by the decomposition of the Zn(*acac*)$_2$, present as a sheath. We feel that the ZnO formed in this manner organizes into energy-minimizing hexagonal structure natural to the würtzite structure. This process also requires a minimum distortion of the surrounding cylindrically formed material. Second, since the core of PVP bundle shrinks away simultaneously, we expect ZnO structure to remain uninfluenced by the PVP (or PVPP).

To examine further whether hydrogen bonding is so extensively involved in the formation of PVP bundles, we have examined the FTIR spectra of the reactants and products of the microwave-induced reactions. We recall that the enolic hydroxyl in PVP itself has a potential for condensation during the irradiation process. The region of interest in the spectra spans from 4000–1400 cm^{-1}. In this region of IR spectra, water has three dominant peaks: at ~3403 cm^{-1} (broad and intense), which corresponds to the symmetric and asymmetric stretching; at 2127 cm^{-1}, which is a combination band due to the bending and librational modes of H–O–H and at 1643 cm^{-1}, which is due to H–O–H bending. Both the bending mode and the stretching mode are sensitive to H-bonding: while the stretching modes exhibit red shifts, the bending mode exhibits a blue shift when there is hydrogen bonding in the system.

The spectra of PVP, [PVP + H_2O], ZnO, after microwave irradiation are shown in figure 6. The spectra of water and alcohol, and that of [PVP + H_2O + Zn(*acac*)$_2$ +

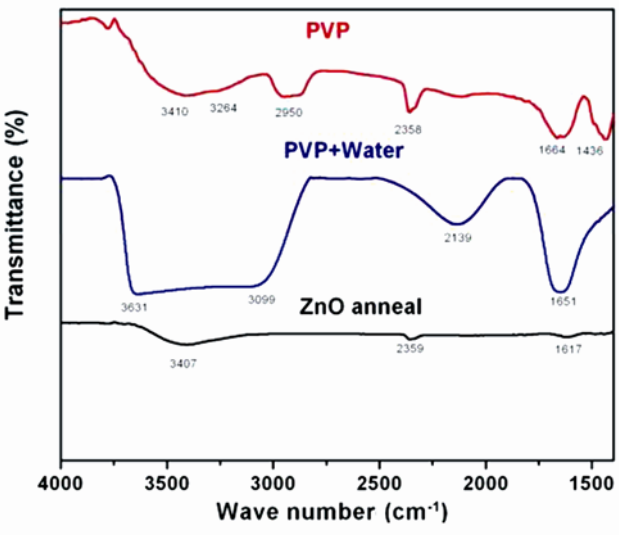

Figure 6. FTIR spectra of PVP, PVP + H_2O and ZnO.

C_2H_5OH], are not shown, as they do not provide any further insight. PVP itself exhibits peaks at 3410 cm^{-1} (with a shoulder on the lower frequency side), at 2359 cm^{-1} and at 1665 cm^{-1}. This is indicative of intra-molecular H-bonding, since the bending mode is clearly at a higher frequency. The C–OH stretching frequency appears to be significantly red-shifted. The spectrum of [PVP + H_2O] is dominated by H_2O absorptions. The broad band at 1652 cm^{-1} is also likely to arise from overlap with blue shifted 1643 cm^{-1} band. The absorption band at 3631 cm^{-1} can be attributed to C–OH stretching, while 3099 cm^{-1} band to the H–OH stretching frequency which is again significantly red-shifted.

The spectrum of the nanorods and nanotubes of ZnO (after heating in air to remove remnant surfactant) has only some surface adsorbed water, and the weak absorption due to water is evident in the spectrum. Thus, the important role played by H-bonding in predisposing ('pre-structuring') the complex of PVP and Zn(*acac*)$_2$ in the presence of water seems to be borne out in the FT–IR spectra.

The role of PVP in the formation of nanostructures is not that of a classical structure-directing agent. Due to its own structure-forming tendency in aqueous solution, PVP effectively provides two different types of scaffolds for the formation of tubes and rods, while it acts as a simple capping agent in forming nanoparticles. We have discounted the participation of ethanol in structure formation, because it is well known that water is far more effective than ethanol as a hydrogen-bonding agent, and also in coupling to microwaves.

4. Conclusions

ZnO nanostructures, such as nanorods and nanotubes, have been synthesized successfully through a very simple microwave-based synthesis technique, from a metal organic complex of zinc. The nanorods and nanotubes have been characterized by X-ray diffraction, scanning electron microscopy and transmission electron microscopy. All the ZnO nanostructures have the same hexagonal würtzite structure and are found to be single crystals of high quality. The growth direction of the ZnO nanorods and nanotubes is found to be [0001] of the würtzite structure of ZnO. A mechanism is proposed and discussed for the formation of nanostructures. It is suggested that formation of supporting assemblies of PVP via extensive hydrogen bonding with imbibed water and also inherent enolic structures gives rise to observed morphologies.

Acknowledgements

The authors acknowledge the Institute of Nanoscience Initiative (INI), a National Facility for Electron Microscopy, Indian Institute of Science, Bangalore, for support in the SEM and TEM analyses reported in this study. One of the authors (SB) also thanks the Council of Scientific and Industrial Research (CSIR), for the award of a research associateship.

References

Arakawa Y and Sakaki H 1970 *Appl. Phys. Lett.* **40** 939
Bilecka I, Djerdj I and Niederberger M 2008 *Chem. Commun.* **7** 886
Bukowski T and Simmons J H 2002 *Crit. Rev. Solid State Mater. Sci.* **27** 119
Edington J W 1976 *Practical electron microscopy in materials science* (New York: Van Nostrand Reinhold Co.) p. 310
Huang M H *et al* 2001 *Science* **292** 1897
Hu Y, Zhou X, Han Q, Cao Q and Huang Y 2003 *Mater. Sci. Eng.* **B99** 41
JCPDS File No – 05-0664
Jian-Feng Y, You-Ming L, Hong-Wei L, Yi-Chun L, Bing-Hui L, Xi-Wu F and Jun-Ming Z 2005 *J. Cryst. Growth* **280** 206
Jung S, Oh E, Lee K, Park W and Jeong S 2007 *Adv. Mater.* **19** 749
Keis K, Magnusson E, Lindström H, Lindquist S E and Hagfeldt A 2002 *Sol. Energy Mater. Sol. Cells* **73** 51
Kim S W, Fujita S and Fujita S 2002 *Appl. Phys. Lett.* **81** 5036
Kong X, Duan Y, Peng P, Qiu C, Wu L, Liu L and Zheng W 2007 *Chem. Lett.* **36** 3
Lao J Y, Huang J Y, Wang D Z and Ren Z F 2003 *Nano Lett.* **3** 235
Lee C J, Lee T J, Lyu S C, Zhang Y, Ruh H and Lee H J 2002 *Appl. Phys. Lett.* **81** 3648
Lee W, Jeong M C and Myoung J M 2004 *Nanotechnology* **15** 1441
Ng H T, Li J, Smith M K, Nguyen P, Cassell A, Han J and Meyyappan M 2003 *Science* **300** 1249
Pan Z W, Dai Z R and Wang Z L 2001 *Science* **291** 1947
Weisbuch C, Benisty H and Houdre´R J 2000 *J. Lumin.* **85** 271
Wu D, Huang L, Wang Q, Zhao X, Li A, Chen Y and Ming N 2006 *Mater. Chem. Phys.* **96** 51
Wu J J and Liu S C 2002 *Adv. Mater.* **14** 215
Xing Y J *et al* 2003 *Appl. Phys. Lett.* **83** 1689
Zhang B P, Binh N T, Wakatsuki K, Segawa Y, Yamada Y, Usami N, Kawasaki M and Koinuma H 2004 *Appl. Phys. Lett.* **84** 4098
Zhou J, Wang Z, Wang L, Wu M, Ouyang S and Gu E 2006 *Superlattices Microstruct.* **39** 314
Zou B, Liu R, Wang F, Pan A, Cao L and Wang Z L 2006 *J. Phys. Chem.* **B110** 12865